Molecular Self-Assembly Inhibition Leads to Basket-Shaped Cyclophane Formation with Chiral Dynamics

Wei Wang,[†,||] Alex D. Bain,[†,‡] Li-Qiong Wang,[†,§] Gregory J. Exarhos,[†,§] and Alexander D. Q. Li*[,†]

Department of Chemistry, Washington State University, Pullman, Washington 99164, Department of Chemistry, McMaster University, Hamilton, ON, Canada L8S 4M1, and Fundamental Science Directorate, Pacific Northwest National Laboratory, Richland, Washington 99354

Received: September 23, 2007; In Final Form: December 20, 2007

Planar perylene derivatives form macrocyclic dimers and concatenated dimer−dimer rings under the action of molecular self-assembly. If this underpinning principle is true, highly twisted perylene derivatives should be more frustrated toward formation of multimeric cyclic compounds such as macrocyclic dimers and concatenated dimer−dimers because of perturbation resulting from intermolecular $\pi-\pi$ stacking. Indeed, 1,6,7,12- tetraphenoxy-substituted perylene is highly twisted and undergoes unimolecular cyclization rather than bimolecular or multimolecular cyclization. The resulting monocyclic monomer exhibits interesting conformation switching from one chiral structure (left-handedness) to another chiral structure (right-handedness) at room temperature. NMR studies of conformational dynamics reveal that such configuration change between the two enantiomers can be frozen at low temperature (−45 °C). An activation enthalpy barrier of 13.4 ± 0.5 kcal·mol^{-1} for twisting the perylene plane in order to convert from one enantiomer to the other has been found.

Introduction

Molecular self-assembly has attracted tremendous interest recently because biological self-assembly processes can generate structures that behave as molecular factories, which are capable of synthesizing specific heterogeneous biopolymers or carrying out sophisticated tasks such as invoking a proton gradient to synthesize adenosine 5′-triphosphate (ATP). In the recent rapid growth of materials chemistry, molecular assembly and supramolecular assembly are often used to generate various diverse nanoarchitectures with targeted physical properties. We would like, however, to emphasize that molecular assembly including dynamic self-assembly can be used to promote certain reaction pathways that will enhance the formation of a particular products otherwise difficult to obtain. Strategies used until now mostly involve template-directed reactions or mechanically interlocked compound synthesis.[1] Electron-rich π-donors and electron-poor π-acceptors can form co-assembled templates[2] that direct the formation of structurally diverse reaction products. Similarly metal-chelated $\pi-\pi$ conjugation directs formation of cyclic and/or concatenated rings.[3] In a previous report,[4] we had studied a large conjugated system, perylene diimide (PDI), and found that $\pi-\pi$ interactions occurred in organic solvents and could be used to direct formation of a macrocyclic PDI dimer and a PDI concatenated dimer−dimer. The hypothesis is that $\pi-\pi$ interactions are the driving force behind the formation of intriguing dimer macrocycles and fascinating concatenated rings. If this hypothesis is correct, twisted PDI derivatives, which can be synthesized by introduction of large substituents at the bay positions (1, 6, 7, and 12 positions of the perylene core) of the perylene skeleton, should be discouraged from forming effective π-stacks, and therefore the reaction products are directed away from the dimer macrocycle and the concatenated structure. Indeed, under the conditions for ring formation, highly twisted PDI, thus, undergoes self-cyclization to form a monocyclic monomer instead of the macrocyclic dimer or the dimer−dimer concatenated structure.

Self-cyclization of 1,6,7,12-tetraphenoxy perylene diimide leads to a chiral cyclophane because perylene bisimides functionalized at the bay positions have been shown to exhibit a twisted skeleton due to electrostatic repulsion and steric interaction between the substituents. Chiral cyclophanes have been extensively studied because they hold impressive promise in the rapidly growing field of chiral separation. In attempts to design generally useful chiral host molecules, Mallouk has synthesized a series of chiral cyclophanes including benzylviologen cyclophanes containing 1,1′-binaphthol[5] and a short amino acid sequence.[6] While early studies on cyclophanes focus on unique electronic properties, beautiful highly symmetric structures, and methodology for cyclophane synthesis,[7] attention has gravitated toward functions and devices in more recent cyclophane studies such as structurally pre-organized ligands for metal ions or chiral auxiliaries or molecular sensors.[8] By use of chiral shifting reagents, Stoddart was able to demonstrate that[2] catenane, consisting of interlocked bisparaphenylene[34] crown-10 and cyclobis-paraquat-*p*-phenylene, existed as mixtures of diastereoisomeric complexes at low temperature (197 K).[9] These studies seem to imply that nontraditional chiral structures, which are generally difficult to distinguish in linear configurations, can be recognized in the cyclophane motif.

Twisted perylene derivatives induce axial chirality (helicity) and undergo rapid dynamic exchange between the two enanti-

* To whom correspondence should be addressed. E-mail: dequan@wsu.edu. Phone: 509-335-7196. Fax: 509-335-8867.
† Washington State University.
‡ McMaster University.
§ Pacific Northwest National Laboratory.
|| Current address: Department of Chemistry, University of California at Davis, One Shields Avenue, Davis, California 95616.

10.1021/jp077650a CCC: $40.75
Published on Web 03/15/2008

CHART 1

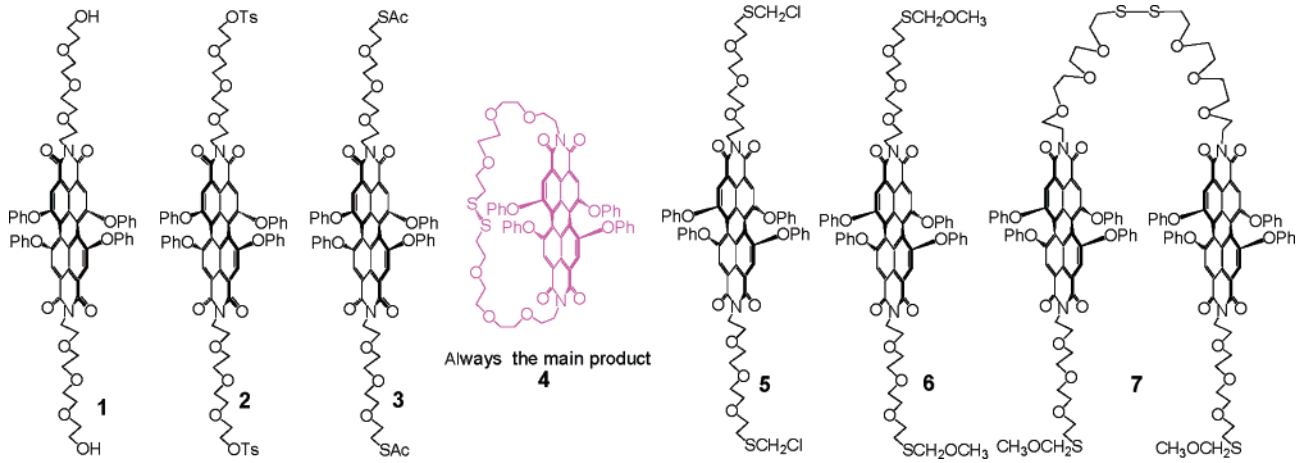

omers in solution. The twisted perylene diimide derivatives have only been observed by X-ray crystallography in the solid state; thus far, the enantiomeric dynamic exchange has not been observed in solution due to the low barrier of rotation. All crystal structures obtained to date crystallize as a racemic mixture containing molecules of both chirality in a 1:1 ratio, and pure isomers in the solid state have not been reported to date. The dihedral twist angle associated with the bay carbon atoms is dependent on the number and type of substituents; the 1,7-difluro-,[10] 1,7-dicyano-,[11] 1,7-dibromo-,[12] 1,6,7,12-tetraphenoxy-,[13] 1,6,7,12-tetrafluoro-,[14] and 1,6,7,12-tetrachloroperylene diimide[15] derivatives have 4, 5, 24, 25, 28/18, 36.7° of twisted dihedral angles, respectively. The distortion from planarity frustrates the packing of these dyes in the solid state as well as in molecular self-assemblies, which affords much more soluble dyes. Incorporation of the twisted chiral perylene diimide into a basket-shaped cyclophane structure, however, has dramatically retarded the dynamic exchange between the two enantiomeric structures. Herein, we rationalize the formation of such a chiral cyclophane in the context of previously reported macrocylic dimer and concatenated dimer−dimer and account for the dynamic interconversion between the two twisted perylene cyclophane enantiomers and the rotation energy barrier separating the pair (Chart 1).

Experimental Section

General Methods. Solvents and reagents were purified using literature methods. Matrix-assisted laser desorption−ionization (MALDI) mass spectra were obtained on an ABVS-2025 spectrometer. Routine ^{1}H NMR spectra were recorded with a Mercury 300 (300 MHz) spectrometer for solutions in $CDCl_3$ (CD_3OD) at ambient temperature. ^{13}C NMR spectra were recorded at 75.48 MHz with a Mercury 300 spectrometer for solutions in $CDCl_3$ (CD_3OD). Bruker 500 and 600 MHz were also used for acquiring special NMR spectra when necessary. Reactions were monitored by thin-layer chromatography (TLC) on precoated plates of silica gel 60 F_{254} (EM Science). Column chromatography was performed on silica gel 60 (230−400 mesh, EM Science) using an eluent as specified in the experiment.

Compound 1: Bis-*N*,*N*′-(2-(2-(2-(2-hydroxyethoxy)ethoxy)-ethoxy)ethyl)-1,6,7,12-tetraphenoxy-3,4,9,10-perylenetetracarboxylic Diimide. To a solution of bis-*N*,*N*′-(2-(2-(2-(2-hydroxyethoxy)ethoxy)ethoxy)ethyl)-1,6,7,12-tetrachloro-3,4,9,10-perylenetetracarboxylic diimide (100 mg, 0.11 mmol) in *N*,*N*-dimethylformide (20 mL) were added potassium carbonate (150 mg, 10 equiv) and phenol (200 mg, 19 equiv) under argon at room temperature (RT). The reaction was continued at 80 °C under argon overnight. The reaction solution was monitored with ^{1}HNMR spectroscopy, which showed completion of the reaction after this amount of time. The solvents were evaporated, and the residue was diluted with $CHCl_3$. The organic phase was washed with 1 N HCl (aq) solution and brine until the aqueous phase became neutral with pH ∼7−8. The organic layer was then dried and concentrated, and the residue was purified by chromatography on a silica gel column eluted with CH_2Cl_2/MeOH (20/1), and the title product, a purple solid, was obtained in a yield of 89% (372 mg): R_f 0.39, CH_2Cl_2/MeOH (20/1). Compound **1**: ^{1}H NMR ($CDCl_3$, 300 MHz) δ 8.19 (s, 4 H, perylene ring), 7.26 (bt, J = 7.2 Hz, 8 H, phenoxy ring), 7.11 (bt, J = 7.2 Hz, 4 H, phenoxy ring), 6.93 (bd, J = 7.2 Hz, 8 H, phenoxy ring), 4.36 (bt, J = 6.0 Hz, 4 H, tetraethylene glycol), 3.76 (bt, J = 6.0 Hz, 4 H, tetraethylene glycol), 3.67−3.50 (m, 24 H, tetraethylene glycol). ^{13}C NMR ($CDCl_3$, 75.48 MHz) δ 163.5, 156.1, 155.5, 133.0, 130.2, 124.8, 122.8, 120.8, 120.3, 120.2, 119.9, 72.7, 70.8, 70.7, 70.5, 70.3, 68.1, 61.9, 39.5. MS (MALDI): m/z 1110.3 $[M]^+$, 1111.3 $[M+H]^+$, 1133.3 $[M+Na]^+$, 1149.3 $[M+K]^+$, 1110.6 $[M]^-$.

Compound 2: Bis-*N*,*N*′-(2-(2-(2-(2-tosylethoxy)ethoxy)-ethoxy)ethyl)-1,6,7,12-tetraphenoxy-3,4,9,10-perylenetetracarboxylic Diimide. To a solution of compound **1** (360 mg, 0.32 mmol) in 25 mL of dry CH_2Cl_2 (4 Å activated molecular sieves, 3 days) at 0 °C was added *p*-toluenesulfonyl chloride (320 mg, 6.3 mmol, 5.2 equiv) and dry triethylamine (NaOH, pellets 3 days) (2.7 mL, 19 mmol). The reaction mixture was then stirred for 2 h at 0 °C and left overnight at room temperature under an argon atmosphere. TLC monitoring showed completion of the reaction. The solvents were evaporated, and the residue was diluted with $CHCl_3$. The organic phase was washed with 1 N HCl (aq) solution and brine until the aqueous phase was pH ∼7−8. The organic layer was dried and concentrated, and the residue was purified by chromatography on a silica gel column eluted with cyclohexane/ethyl acetate (2/3), and the title product as a purple syrup was obtained with a yield of 82% (372 mg): R_f 0.21, cyclohexane/ethyl acetate (2/3). Compound **2**: ^{1}H NMR ($CDCl_3$, 300 MHz) δ 8.18 (s, 4 H, perylene ring), 7.76 (d, J = 8.4 Hz, 4 H, tosyl aromatic ring), 7.31 (bd, J = 8.4 Hz, 4 H, tosyl aromatic ring), 7.26 (bt, J = 7.2 Hz, 8 H, phenoxy ring), 7.11 (bt, J = 7.2 Hz, 4 H, phenoxy ring), 6.93 (bd, J = 7.2 Hz, 8 H, phenoxy ring), 4.35 (bt, J = 6.0 Hz, 4 H, tetraethylene glycol), 4.11 (bt, J = 4.8 Hz, 4 H, tetraethylene glycol), 3.74 (bt, J = 6.0 Hz, 4 H, tetraethylene glycol), 3.64−3.60 (m, 8 H, tetraethylene glycol),

3.58−3.48 (m, 12 H, tetraethylene glycol). ^{13}C NMR ($CDCl_3$, 75.48 MHz) δ 163.3,155.8, 155.3, 144.7, 132.9, 132.8, 130.0, 129.8, 128.0, 124.6, 122.5, 120.6, 120.1, 120.0, 119.6, 70.68, 70.57, 70.48, 70.0, 69.2, 68.6, 67.8, 39.3, 21.6. MS (MALDI): *m/z* 1418.46 $[M]^+$, 1419.53 $[M+H]^+$, 1441.47 $[M+Na]^+$, 1418.3 $[M]^-$.

Compound 3: Bis-*N,N′*-(2-(2-(2-(2-thioacetylethoxy)-ethoxy)ethoxy)ethyl)-1,6,7,12-tetraphenoxy-3,4,9,10-perylenetetracarboxylic Diimide. To a solution of compound **2** (286 mg, 0.2 mmol) in *N,N*-dimethylformide (60 mL) was added potassium thioacetate (370 mg, 3.2 mmol, 15.6 equiv), and the mixture was stirred at 80 °C under an argon atmosphere overnight. The mixture was then concentrated under decreased pressure and purified by chromatography on a silica gel column eluted with cyclohexane/ethyl acetate (2/3). Compound **3** was obtained as a dark purple solid with a yield of 73% (180 mg). R_f 0.37, cyclohexane/ethyl acetate (2/3). Compound **3**: ^{1}H NMR ($CDCl_3$, 300 MHz) δ 8.19 (s, 4 H, perylene ring), 7.26 (bt, J = 7.2 Hz, 8 H, phenoxy ring), 7.11 (bt, J = 7.2 Hz, 4 H, phenoxy ring), 6.93 (bd, J = 7.2 Hz, 8 H, phenoxy ring), 4.36 (bt, J = 6.0 Hz, 4 H, tetraethylene glycol), 3.75 (bt, J = 6.0 Hz, 4 H, tetraethylene glycol), 3.67−3.62 (m, 4 H, tetraethylene glycol), 3.62−3.50 (m, 16 H, tetraethylene glycol), 3.03 (t, J = 6.4 Hz, tetraethylene glycol), 2.29 (s, 6 H, $-COCH_3$). ^{13}C NMR ($CDCl_3$, 75.48 MHz) δ 195.5, 163.3, 155.8, 155.3, 132.8, 130.0, 124.6, 122.6, 120.6, 120.1, 120.0, 119.6, 70.6, 70.5, 70.3, 70.1, 69.7, 67.8, 39.3, 30.5, 28.8. MS (MALDI): *m/z* 1226.4 $[M]^+$, 1227.5 $[M+H]^+$, 1249.4 $[M+Na]^+$, 1226.4 $[M]^-$.

General Procedure for Unimolecular Cyclization: Formation of Perylene Cyclophane, 4. De-acetylation was carried out by adding NaOMe (2 M in MeOH) dropwise to a solution of thioacetyl compound **3** in CH_2Cl_2, 4 drops (9" Pasteur pipet) for every 100 mL of solution at RT. The color of the reaction mixture changed from purple to dark blue. TLC detection was conducted, and the reaction was then neutralized with Amberlite IR-120 (H^+) resin upon the disappearance of the starting material. The mixture was filtered, and the filtrate was concentrated and flash chromatographed (SiO_2, CH_2Cl_2/MeOH) to give the final products as described below.

Compound **3** at concentrations of 0.57 mM and 0.1 mM, respectively, was used in the starting synthesis, and compound **4** (bis-*N,N′*-(2-(2-(2-(2,2′-dithioethoxy)ethoxy)ethoxy)ethyl)-36-crown-6-(1,6,7,12-tetraphenoxy-3,4,9,10-perylenetetracarboxylic diimide)) was obtained as the main product in 55 and 40% yield. Compound **5** (bis-*N,N′*-(2-(2-(2-(2-(chloromethylthio)-ethoxy)ethoxy)ethoxy)ethyl)-1,6,7,12-tetraphenoxy-3,4,9,10-erylenetetracarboxylic diimide), a chloromethyl thiol ether of **3** as a byproduct with a yield of 35%, was formed in the same reaction and isolated following purification. Before quenching the reaction with Amberlite, further reaction drives formation of compound **6** (bis-*N,N′*-(2-(2-(2-(2-(methoxymethylthio)ethoxy)ethoxy)ethoxy)ethyl)-1,6,7,12-tetraphenoxy-3,4,9,10-perylenetetracarboxylic diimide), a methoxy thiol ether, that forms from compound **5** with a yield of 30% following methanol addition to the solution. As a byproduct, a linear dimer of compound **6**, compound **7** (2,2′-bis-[2-[2-[2-(2-(2-(2-methoxymethylthioethoxy)ethoxy)-ethoxy)ethyl)imido-1,6,7,12-tetraphenoxyperyleneimidoethoxy]-ethoxy]-ethoxy]ethyl disulfide) was also found in trace amounts (5%). Compound **4**, TLC, R_f 0.21, cyclohexane/ethyl acetate (2/3). ^{1}H NMR ($CDCl_3$, 300 MHz, at room temperature; see text for variable-temperature ^{1}H NMR) δ 8.20 (s, 4 H, perylene ring), 7.27 (bt, J = 7.5 Hz, 8 H, phenoxy ring), 7.11 (bt, J = 7.5 Hz, 4 H, phenoxy ring), 7.00−6.90 (m, 8 H, phenoxy ring), 4.46−4.34 (m, 4 H, tetraethylene glycol), 3.83−3.75 (m, 4 H, tetraethylene glycol), 3.58−3.46 (m, 4 H, tetraethylene glycol), 3.33 (t, J = 4.8 Hz, 4 H, tetraethylene glycol), 3.16 (t, J = 6.3 Hz, 4 H, tetraethylene glycol), 3.08−2.99 (m, 4 H, tetraethylene glycol), 2.28 (t, J = 6.3 Hz, 4 H, tetraethylene glycol). ^{13}C NMR ($CDCl_3$, 75.48 MHz) δ 163.3, 155.9, 155.3, 132.9, 130.0, 124.7, 122.6, 120.5, 120.0, 119.98, 119.6, 71.08, 70.55, 70.43, 70.3, 69.0, 67.7, 39.7, 37.4. MS (MALDI): *m/z* 1140.3 $[M]^+$, 1141.3 $[M+H]^+$, 1263.3 $[M+Na]^+$, 1140.4 $[M]^-$. Compound **5**: TLC R_f 0.57, cyclohexane/ethyl acetate (2/3). ^{1}H NMR ($CDCl_3$, 300 MHz) δ 8.19 (s, 4 H, perylene ring), 7.27 (bt, J = 8.4 Hz, 8 H, phenoxy ring), 7.11 (bt, J = 8.4 Hz, 4 H, phenoxy ring), 6.93 (bd, J = 8.4 Hz, 8 H, phenoxy ring), 4.75 (s, 4 H, $-SCH_2Cl$), 4.36 (t, J = 6.0 Hz, 4 H, tetraethylene glycol), 3.75 (t, J = 6.0 Hz, 4 H, tetraethylene glycol), 3.69 (t, J = 6.3 Hz, 4 H, tetraethylene glycol), 3.67−3.52 (m, 16 H, tetraethylene glycol), 2.87 (t, J = 6.3 Hz, tetraethylene glycol). ^{13}C NMR ($CDCl_3$, 75.48 MHz) δ 163.3, 155.8, 155.3, 132.8, 130.0, 124.6, 122.6, 120.6, 120.1, 120.0, 119.6, 70.61, 70.56, 70.41, 70.37, 70.2, 67.8, 50.1, 39.3, 30.9. MS (MALDI): *m/z* 1237.7 $[M]^+$, 1238.7 $[M+H]^+$, 1237.65 $[M]^-$. Compound **6**: TLC R_f 0.32, cyclohexane/ethyl acetate (2/3). ^{1}H NMR ($CDCl_3$, 300 MHz) δ 8.19 (s, 4 H, perylene ring), 7.27 (bt, J = 8.4 Hz, 8 H, phenoxy ring), 7.11 (bt, J = 8.4 Hz, 4 H, phenoxy ring), 6.93 (bd, J = 8.4 Hz, 8 H, phenoxy ring), 4.60 (s, 4 H, $-SCH_2OCH_3$), 4.36 (t, J = 6.0 Hz, 4 H, tetraethylene glycol), 3.75 (t, J = 6.0 Hz, 4 H, tetraethylene glycol), 3.66−3.52 (m, 20 H, tetraethylene glycol), 3.30 (s, 6 H, $-SCH_2OCH_3$), 2.73 (t, J = 6.9 Hz, tetraethylene glycol). ^{13}C NMR ($CDCl_3$, 75.48 MHz) δ 163.3, 155.8, 155.3, 132.8, 130.0, 124.6, 122.6, 120.6, 120.1, 120.0, 119.6, 75.8, 70.99, 70.60, 70.55, 70.22, 70.1, 67.8, 55.7, 39.3, 30.3. The assignment was based on HMQC experiment. MS (MALDI): *m/z* 1230.4 $[M]^+$, 1253.4 $[M+Na]^+$, 1269.4 $[M+K]^+$, 1230.4 $[M]^-$. Compound **7**: TLC R_f 0.29, cyclohexane/ethyl acetate (2/3). ^{1}H NMR ($CDCl_3$, 300 MHz) δ 8.180 (s, 4 H, perylene ring), 8.177 (s, 4 H, perylene ring), 7.26 (bt, J = 7.5 Hz, 16 H, phenoxy ring), 7.11 (bt, J = 7.5 Hz, 8 H, phenoxy ring), 6.93 (bd, J = 7.5 Hz, 16 H, phenoxy ring), 4.60 (s, 4 H, $-SCH_2OCH_3$), 4.38−4.31 (m, 8 H, tetraethylene glycol), 3.79−3.70 (m, 8 H, tetraethylene glycol), 3.68−3.50 (m, 40 H, tetraethylene glycol), 3.30 (s, 6 H, $-SCH_2OCH_3$), 2.80 (t, J = 4.8 Hz, 4 H, tetraethylene glycol), 2.73 (t, J = 4.8 Hz, 4 H, tetraethylene glycol). MS (MALDI): *m/z* 2370.8 $[M]^+$, 2393.7 $[M+Na]^+$, 2409.8 $[M+K]^+$, 2370.8 $[M]^-$.

Results and Discussion

Frustration of Molecular Self-Assembly Directs a Unimolecular Cyclization Reaction. Planar perylene molecules attract each other and form π-stacks. The $\pi-\pi$ interactions are reinforced in aqueous systems by hydrophobic interactions resulting in folded systems that are hyperthermophilic (heat-loving).[16] However, such strong self-organization phenomena cannot be fully taken advantage of because current organic chemistry techniques show limited success in aqueous systems. Fortunately, $\pi-\pi$ interactions also occur in organic solvents that include chlorinated solvents. As a result, the solution of a simple planar perylene derivative has an impressive series of self-organized nanostructures including self-assembled dimer, trimer, tetramer, and higher oligomers. One practical treatment assumes that the equilibrium constants (K) between self-assembled n-mer and (n+1)-mer (n = 1, 2, 3, etc.) all have essentially the same value and are equal to each other, leading to the equal-K model. In chloroform or methylene choloride, the equilibrium constant was determined to be $K = 52\ M^{-1}$ for

SCHEME 1[a]

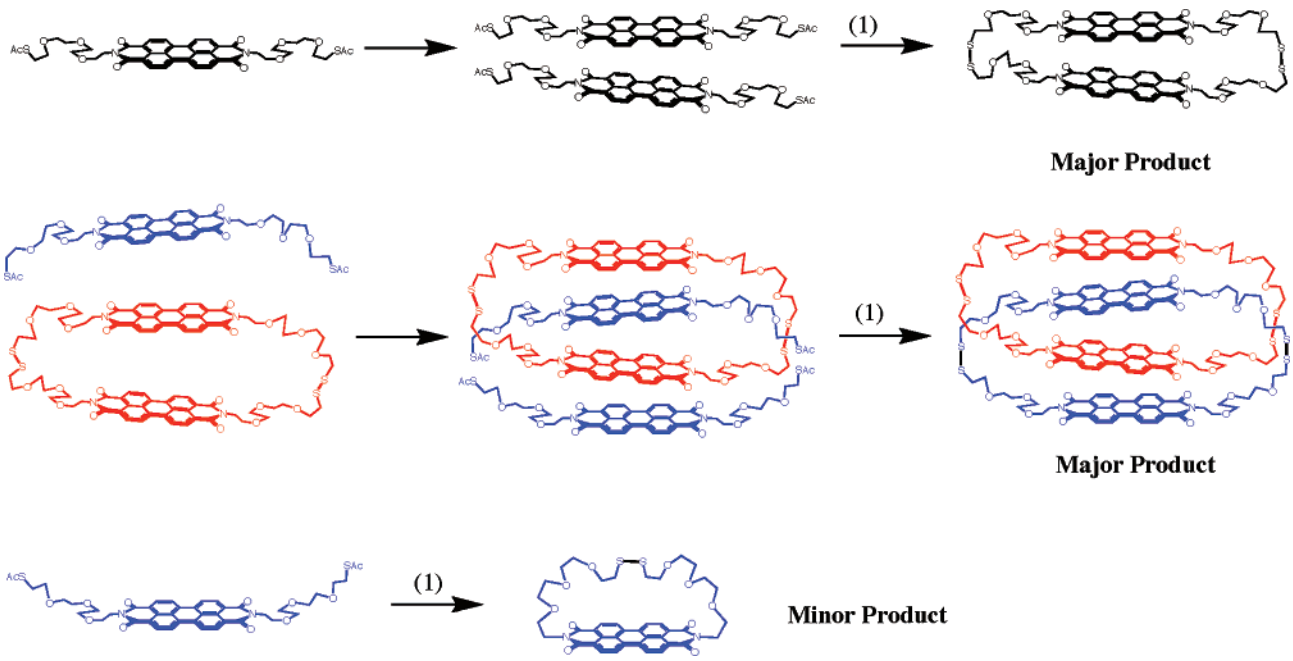

[a] Conditions: (1) NaOM/MeOH, open to air, at rt.

SCHEME 2[a]

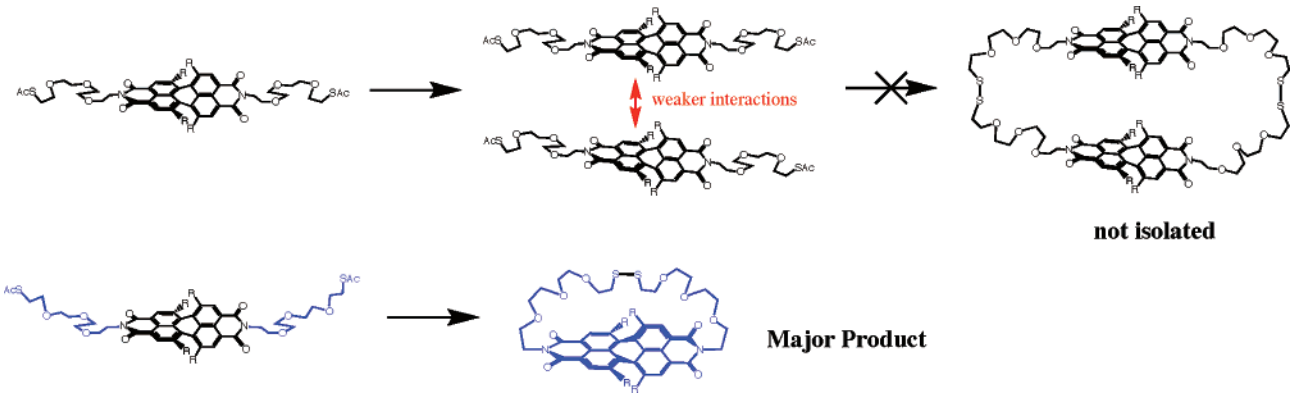

[a] Conditions: (1) NaOM/MeOH, open to air, at rt.

bis-*N*,*N*′-(2-(2-(2-ethoxy)ethoxy)ethoxy)ethyl)perylenetetracarboxylic diimide, indicating that planar perylene derivatives form spontaneous self-assembled oligomers (SAO).[17] These SAOs will affect the physical properties as well as chemical reactivities and reaction pathways. Indeed, activation of the terminal function groups of bis-*N*,*N*′-(2-(2-(2-(2-thioacetylethoxy)ethoxy)ethoxy)ethyl)perylenetetracarboxylic diimide results predominantly in major products of the macrocyclic dimer and interlocked dimer−dimer rings (Scheme 1).

However, frustration of intermolecular self-assembly should divert reaction pathways away from the self-assembled products such as the macrocyclic dimer and interlocked dimer−dimer rings. While intermolecular reactions are discouraged, intramolecular reactions are favored, which lead to unimolecular cyclization as shown in Scheme 2. It is instructive to compare Schemes 1 and 2. The reactive groups in both cases are thioacetyl, and the reaction is the hydrolysis of thioesters, yielding an active thiol-like intermediate species that forms disulfide bonds. The distance between the two thioacetyl groups within the reaction precursor is the same in both cases (planar or twisted perylenes), roughly 39 Å away. The nanoenvironment of the reaction centers is the same because both are bound to tetraethylene glycol linkers. Therefore, it is inconceivable to consider any electronic effects such as electron induction or hyperconjugation from the perylene unit (through bond effects) could contribute to the reactivity or alter the course of the reaction. Since the reaction center is ∼14 Å away from the perylene unit, it is also unlikely that perylene could induce any steric repulsion (through space effects) unless molecular self-assembly could be invoked.

Twisting the perylene core does not affect the electronic nature of the reaction center at the thioacetyl groups nor does it introduce any appreciable steric effect within the proximity of the reaction centers. The question arises as to why two very similar reactants could lead to such dramatically different results: one yields a macrocylic dimer (yield 39%) and concatenated dimer−dimer rings (yield 36%) as the major products (total yield: 75%), and the other yields an unimolecular cyclophane as the major product (yield 40−55%) along with linear byproducts (yield 35%) with a total yield up to 90%.

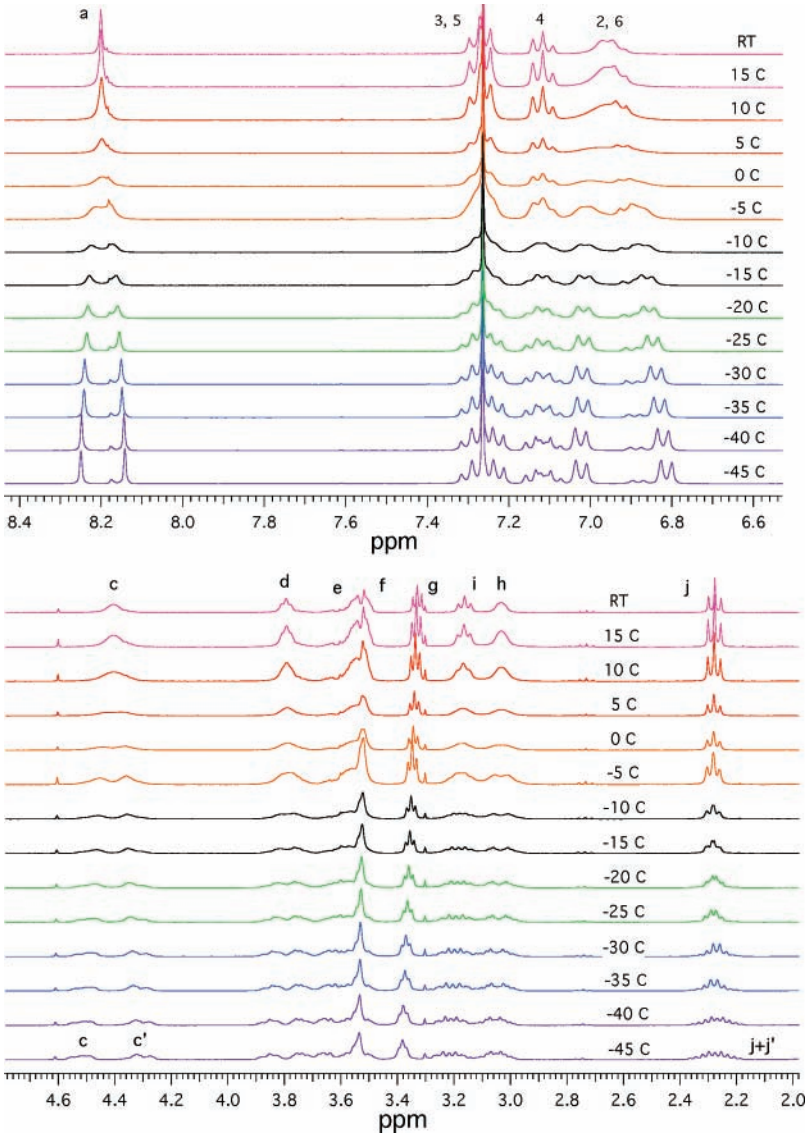

Figure 1. Variable-temperature ^{1}H NMR spectra of perylene diimide cyclophane (**4**) with the aromatic proton region shown on the top panel and the aliphatic region shown on the bottom panel.

Herein, we attribute these observed phenomena to molecular self-assembly effects. In other words, the presence of molecular self-assemblies in a reaction system can completely alter the course or pathways of the reaction, and sometimes these new reaction pathways could lead to novel structures such as interlocked rings that are otherwise difficult to obtain through normal reaction design.

When the self-assembly pathways are frustrated, the reaction chooses those secondary reaction options. On the basis of the reaction conditions, deacetylation took place first, and the formation of byproduct compound **5** indicated the existence of thiolate R-S$^-$ as an active intermediate (see Supporting Information Figure 1, which shows that compound **5** was a S_{N2} replacement of CH_2Cl_2). Because the twisted perylene core frustrated self-organization, the thiol-like intermediate was directed away from the macrocyclic dimer and the concatenated dimer−dimer. As a result, the reaction was limited to unimolecular cyclization as well as reactions with secondary reagents such as the solvent. Indeed, compound **5** (35%), a product of the reaction between R-S$^-$ intermediate and solvent CH_2Cl_2, and compound **4** (55%), the major product from the intramolecular disulfide formation via oxidation of R-S$^-$ intermediate by air, were formed due to random collision in solution rather than self-assembly-directed reactions. The formation of compound **6** (30%) from compound **5** after the addition of the polar solvent methanol also indicated the solvation effect on the twisted starting material; the two thiol ends of the molecule on the tetraethylene glycol linkers have stretched apart and reacted randomly (Supporting Information Figure 1, which shows that compound **6** was from a S_{N2} reaction between compound **5** and methoxide). In addition, a trace amount of compound **7** was isolated and characterized as a linear dimer structure, also formed via random collision of the R-S$^-$ intermediate as evidenced by the low yield (<5%). Comparably the formation of monocyclic cyclophane **4** was more favored because of the intramolecular pathway; it has a higher yield than the linear dimer (5%) and solvation product (35%).

Interconversion Dynamics between the P and M Helical Enantiomers. The resulting chiral cyclophane (Scheme 2; compound **4**) is characterized by advanced NMR techniques including correlation spectroscopy (COSY), gradient-enhanced nuclear overhauser effect spectroscopy (GOESY), and variable-temperature experiments. From the COSY experiment, the chemical shift (δ) of protons on tetraethylene glycol chains as well as perylene aromatic rings can be assigned as follows ($CDCl_3$, 300 MHz, at room temperature) (Figure 1 and Scheme

SCHEME 3

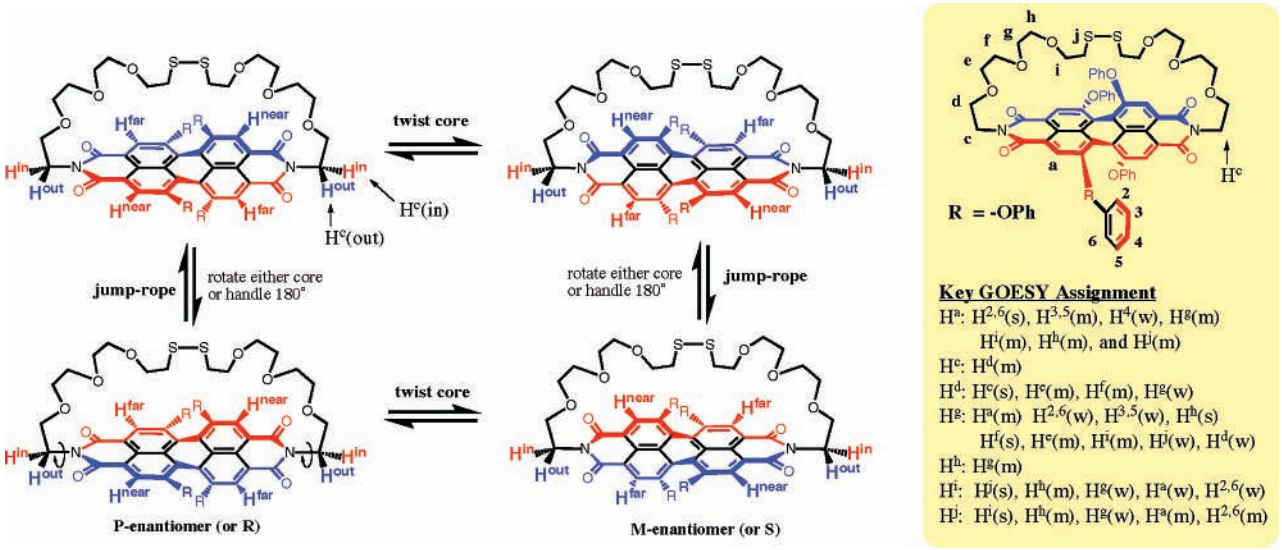

3): protons on perylene ring, H^a (8.20); protons on phenoxy rings, Ar−$H^{3,5}$ (7.27), Ar−H^4 (7.11), Ar−$H^{2,6}$ (7.00−6.90); protons on ethylene glycol chains, H^c (4.46−4.34), H^d (3.83−3.75), $H^{e,f}$ (3.58−3.46), H^g (3.33), H^h (3.08−2.99), H^i (3.16), and H^j (2.28).

The 1D GOESY experiments, which are more sensitive than 2D nuclear overhauser effect (NOE) such as NOESY or rotational nuclear overhauser effect spectroscopy (ROESY), clearly showed the spatial correlation between H^a and H^j, supporting that they are spatial neighbors although non-neighboring through covalent bonds; this suggests that compound **4** has a basket-shaped structure. Details of the GOESY analyses were listed in Scheme 3. In the GOESY experiments, when proton H^a was irradiated, the radiation energy absorbed by protons H^a could be transferred to its neighbors through space, emphasizing the spatial co-relationship of nearby nuclei. Thus, as shown in Scheme 3, H^a protons had strong correlations (s: strong signature) with the 2,6-protons on phenoxy H,[2,6] which is expected because they are neighbors linked through covalent bonds. However, H^a protons also had medium-strength coupling (m: medium signature) to the protons on the "handle" of the basket such as H^g, H^i, H^h, and H^j through space as well as to the next-nearest neighbors on the phenoxy ring through covalent bonds, the protons at the 3 and 5 positions H.[3,5] These results indicate that the handle protons H^g, H^i, H^h, and H^j are as close to proton H^a as the phenoxy proton H,[3,5] which is only ∼4.85 Å away from H^a. This only happens when the compound forms a basket structure and when the results of GOESY assignments of H^g, H^i, H^h, and H^j protons being spatial neighbors of proton H^a corroborate with a basket-shaped molecular structure. Finally, weak correlation (w: weak signature) was observed between H^4 and H^a, indicating that protons H^a are closer to H^g, H^i, H^h, and H^j protons than to the proton at the 4-postion of the phenoxy ring, H^4. The AM1 energy minimized geometry shows that the distances between H^a and $H^{2,6}$, $H^{3,5}$, and H^4 are on average 3.39, 4.85, and 5.37 Å, respectively. By use of these data as a calibration, the GOESY experiments suggest that the handle protons float above the basket with an average distance from proton H^a greater than 3.39 Å but closer than 5.37 Å. These results are in agreement with AM1 simulations that showed the H^i protons could move as close as 3.74−4.19 Å away from protons H^a.

The uniqueness of the basket-shaped cyclophane is that it enables the observation of interconversion between the P-enantiomer, which is a right-handed helix and equivalent to the R configuration, and M-enantiomer, which is a left-handed helix and equivalent to the S configuration. In Figure 1, variable-temperature ^{1}H NMR shows that, in this dynamic exchange process, the aromatic protons yield a relatively sharp peak at 20 °C, but the peak coalesces at 0 °C and further splits into two peaks at low temperature. The experimental results indicate that the two types of protons (H^a_{near} defined as the aromatic proton *near* the TEG handle and H^a_{far} defined as the aromatic proton *far* away from the TEG handle) must undergo a rapid exchange at RT, and this process can be frozen at low temperatures. At ambient temperature, the NMR spectrum indicated a symmetrical molecule, and we observed an averaged effect of H^a_{near} and H^a_{far}; however, cooling the sample to −45 °C caused the lines in the spectrum to broaden and then split into two equally intense lines, as seen in Figure 1. This indicates that the molecule has two equivalent conformations, which exchange quickly at ambient temperature; but the process can be frozen out at −45 °C. This is not surprising, since a crystal structure[18] of molecules resembling the perylene core shows that the molecules are not planar but twisted around their long axes. Steric hindrance of the *O*-phenyl groups may well be responsible, by analogy to ortho-substituted biphenyls, which show similar twisting. The presence of the cyclophane "handle" over the perylene "basket" renders the two twisted forms inequivalent, so when the exchange is slow, we see both enantiomers.

What is the process that interconverts the two forms? There are two hypothetical mechanisms that can cause proton H^a exchange. One exchange mechanism is an inversion of the internal twist in the perylene core, which interconverts the P-enantiomer to the M-enantiomer (Scheme 3). The other mechanism involves swinging the TEG handle from one face of the perylene to the opposite face like a jump rope; this mechanical process is equivalent to rotating the *rigid* perylene core while holding the twisting motion still. Thus, it does not interconvert one enantiomer to the other (Scheme 3) since the perylene core has an approximate C_2 symmetry along its long axis. However, this process does interconvert H^a_{near} with H^a_{far}, similar to the exchange between the axial protons and equatorial protons in cyclohexane. Of key importance is verifying that the experimental results can be interpreted in terms of the twisting of the perylene core mechanism, not the jump rope mechanism. The jump rope dynamic process switches the protons (H^a_{far} ↔

H^a_{near}) but leaves proton H^c in the same environment in the initial and final states, whereas the perylene skeleton inversion dynamics switches both H^a and H^c protons.

The molecular jump rope (or skipping rope) in planar chiral cyclophanes has been reported before, and with the assistance of a chiral auxiliary group, the planar chiral cyclophanes prefer one diastereomer over the other.[19] In fact, a chiral cyclophane consisting of a benzene ring and an indole unit can also undergo similar dynamics, in which the indole unit flips 180°. This process has an energetic barrier of $\Delta G^{\ddagger} = 10.9 \pm 0.2$ kcal/mol for indole ring flipping from one enantiomer to the other enantiomer, according to the Gutowsky−Holm equation and variable-temperature NMR measurements.[20] However, in our basket-shaped chiral cyclophane system, the jump rope mechanism does not occur. If the perylene core were not twisting at RT, the c and c′ protons would be distinguishable since one proton feels a neighboring carbonyl next to the H^a_{far} and the other feels a neighboring carbonyl next to H^a_{near}. Such arrangement would result in two groups of chemical resonances for c and c′ protons, respectively, at RT, and this is contrary to the experimental data. As we lower the temperature, the jump rope mechanism leads the c proton to the same c proton and the c′ proton to the same c′ proton. Therefore, the two groups of chemical resonances would remain the same assuming that the NMR spectrum is only sensitive to the initial and final states. Experimentally, we observed a broad singlet peak instead of two groups of peaks, which collapse at 0−5 °C and further collapse at −15 °C. Analyses of H^c protons rules out the jump rope mechanism at RT or low temperature. At high temperature, the jump rope mechanism may be as probable as the twisting core mechanism leading to coupling and associated complex dynamics. But if this hypothesis is true, experimental data suggest that the jump-rope mechanism freezes well before the twisting core mechanism stops actuating; therefore the energy barrier measured at temperatures between 0 to −5 °C associates with twisting the perylene core.

Therefore, the interconversion of the perylene protons must be due to the twisting perylene core mechanism. At RT, twisting of the perylene core not only interconverts H^a_{near} and H^a_{far} but also exchanges H^c and $H^{c'}$. As a result, the c proton resonance is a broad singlet at RT, which is in agreement with experimental observations. When the twisting is frozen, the c and c′ protons will be distinguishable and magnetically inequivalent; this is exactly what was observed experimentally. The argument for a twisting mechanism is also supported by a detailed interpretation of the spectra as the perylene core and phenoxy groups are moving in a concerted process. This is supported by an analysis of the protons labeled "a" and the protons on the phenyl groups. The H^a protons are a classic case of two-site equally populated exchange,[21−23] so it is easy to extract rate measurements from the spectra in Figure 2. The phenyl protons are coupled and so must be analyzed by density matrix methods,[24,25] but this is straightforward. Within experimental error, the rate of exchange for the phenyl protons is the same as the H^a protons, which strongly suggests a concerted process among the aromatic cores.

Figure 2 also shows simulated spectra using the standard Gutowsky−Holm equations for two-site equally populated chemical exchange interactions. Rates were adjusted to give the best fit to the spectra, and these rates were used to create an Eyring plot in Figure 3. The H^a protons provide the most convenient measure of the rate as a function of temperature from −10 to +15 °C. The Eyring plot of ln(rate/T) against (1/T) is shown in Figure 3. The data are not sufficient to provide a reliable entropy of activation, but the enthalpy of activation can

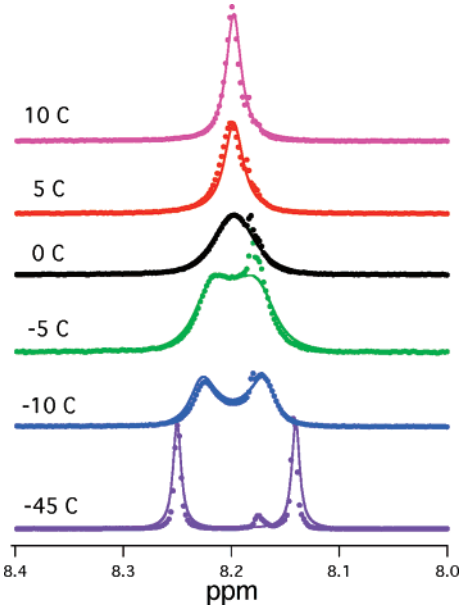

Figure 2. Simulation of the aromatic proton H^a (solid line) are plotted along with experimental NMR spectra (solid circles). The simulation yields dynamic exchange rates between H^a_{far} and H^a_{near} due to twisting of the perylene core.

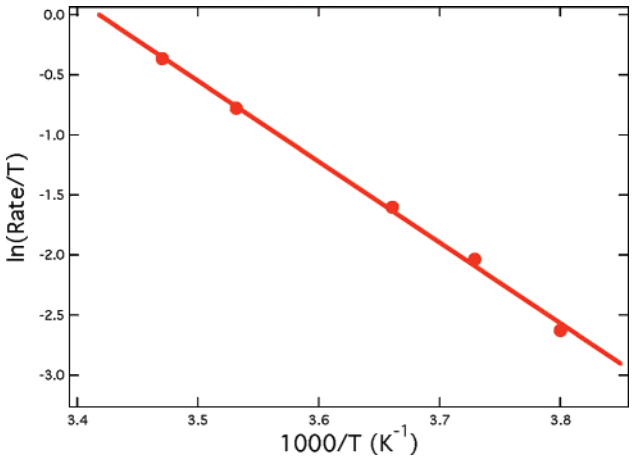

Figure 3. Eyring plot. Eyring plot of ln(rate/T) vs 1000/T. The slope of the line is $-\Delta H^{\ddagger}/R$, where the enthalpy of activation $\Delta H^{\ddagger}$ for the twisting perylene core is determined to be 13 kcal/mol.

be obtained from the slope of the line. We obtain an energy barrier value between the P and M enantiomers of 13.4 ± 0.5 kcal·mol^{-1}, which represents the energy required to twist the perylene core with tetraphenoxy substitutions at 1, 6, 7, and 12 positions.

The ambient temperature spectrum in Figure 1 suggests that the molecule rapidly flips between conformations. The g and j protons are magnetically equivalent and reveal equal couplings to their neighbors, as shown by their triplet structure. However, the protons labeled c and j offer further insight into the dynamics. Both these sets of protons comprise CH_2-CH_2 units, but the c protons are at the junction of the handle and the basket, whereas the j protons are in the middle of the handle. The difference in dynamics can be seen in the spectra at −45 C.

In an asymmetric molecule, all four protons in a rigid CH_2-CH_2 unit are magnetically inequivalent. The two protons in each CH_2 group will show two eight-line splitting patterns; each proton is split into a doublet of doublets of doublets by the three other protons in the group. Figure 4 shows this clearly for the c protons. The top half of Figure 4 also shows, with simulated

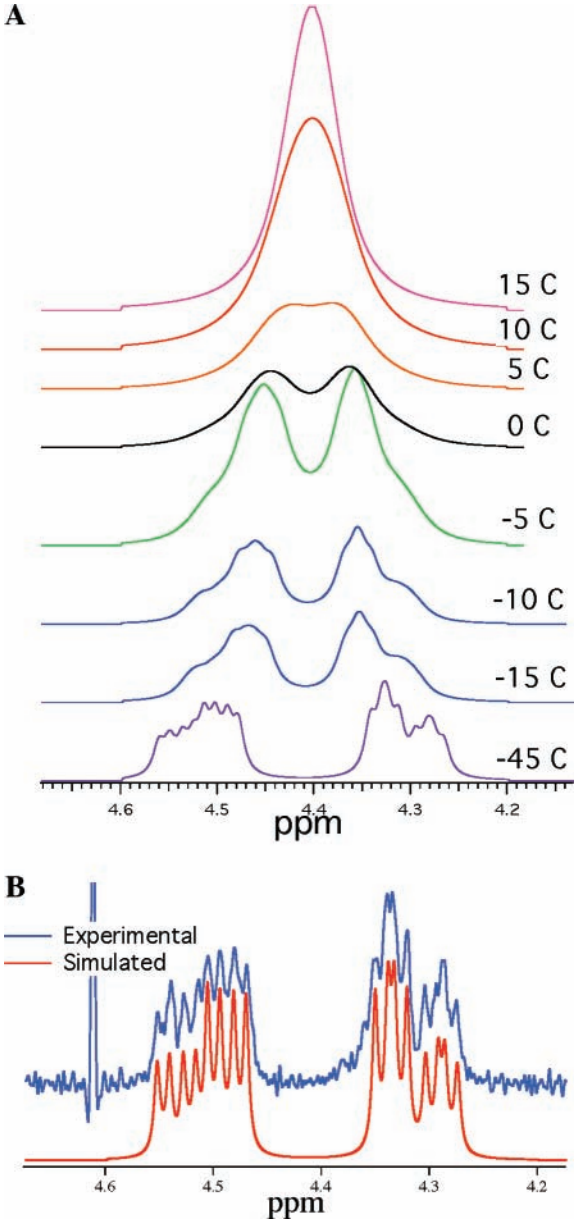

Figure 4. (A) Simulated spectra of the c and c′ protons as a function of temperature. (B) Resolution-enhanced version of the −45 °C spectrum, along with a spin simulation. The doublet-of-doublets-of-doublets (8 peaks) structure of each proton line indicates that the vicinal couplings are all different and that the system is relatively rigid.

spectra, what happens to this spectrum as chemical exchange speeds up. The spectra all use the same chemical shifts and couplings, only the rate of exchange (taken from Figure 2) has changed. We do not have stereospecific assignments, but the high-frequency (low-field) "c" proton has couplings of 3.4 and 7.3 Hz, whereas the low-frequency (high-field) component has couplings of 3.5 and 5.3 Hz. The chemical shift difference between c and c′ is roughly 0.02 ppm but is temperature dependent, and the geminal coupling is −14 Hz. This indicates that the dihedral angles are different, suggesting a relatively fixed geometry with little motion around carbon−carbon bond. Since this part of the chain is relatively rigid, the four vicinal couplings between the c protons and the d protons are all different: 3.4, 3.5, 5.3, and 7.3 Hz.

By contrast, the spectra of the j protons show a different dynamic behavior. The bottom part of Figure 5 shows the analysis of the somewhat-confusing band that represents the two j protons. If the two j protons were isolated, they would form

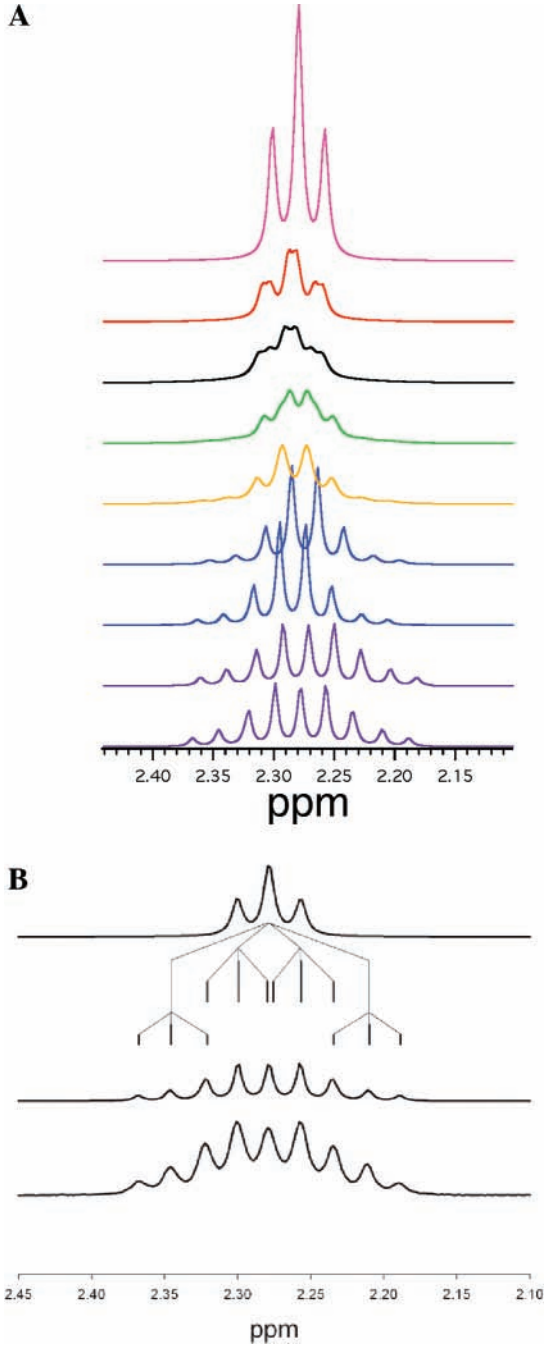

Figure 5. (A) Simulated spectra of the j and j′ protons as a function of temperature. (B) The top simulated trace shows the fast exchange triplet from j and j′ protons at high temperatures. When the exchange stops, j and j′ protons split each other into two doublets with distorted intensities but always retain the triplet structure, resulting the middle trace simulated pattern, which matches well to the bottom trace, which is the experimental spectrum at −45 °C.

an AB-type pattern. Each of the j protons is split into a doublet by their mutual geminal coupling (again, approximately −14 Hz), but the intensities are strongly distorted by second-order effects, caused by the fact that the j and j′ chemical shifts are very close. In the actual spectrum, each of these lines is further split into a doublet of doublets by the two i protons. However, these coupling constants are equal within experimental resolution, so the doublet of doublets collapses to a 1:2:1 triplet, as shown in Figure 5. The analysis is further complicated by the overlap of some of the lines, to give the 9-line pattern in Figure 5, and by the fact that, at a higher temperature, the temperature-dependent chemical shift difference turns the 9-line pattern into

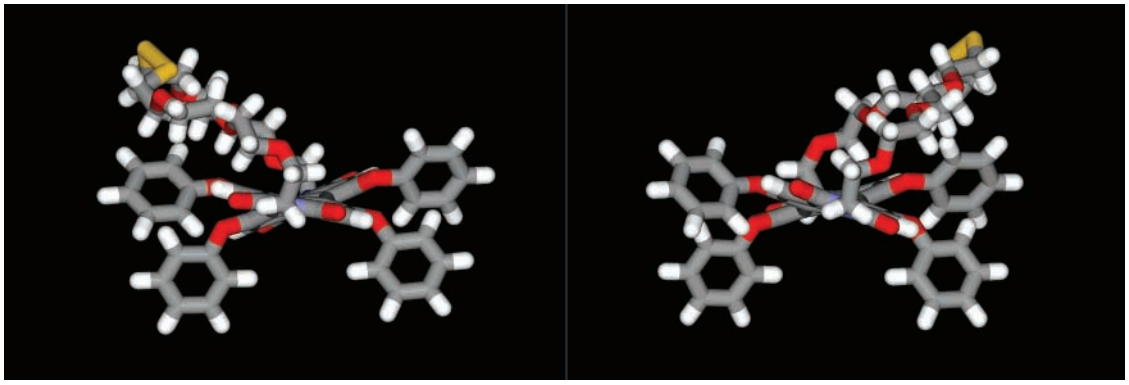

Figure 6. After the twisting motion of the perylene core is frozen ($T < -5$ °C), the flexible handle can still flop left and right as evidenced by the clearly resolved triplet of the j and g protons. However, such motions are significantly reduced below −15 °C, concomitant with further splitting of triplet j proton pattern to the intensity-distorted doublet−doublet pattern (i.e., the emergence of j and j′ magnetic inequivalence). AM1 geometry minimized structures show the handle flop left (left) and right (right). Note since the twisting is frozen, the flopping process results in the same identical molecules rather than enantiomers, but this process does exchange the geminal protons such as j and j′.

SCHEME 4[a]

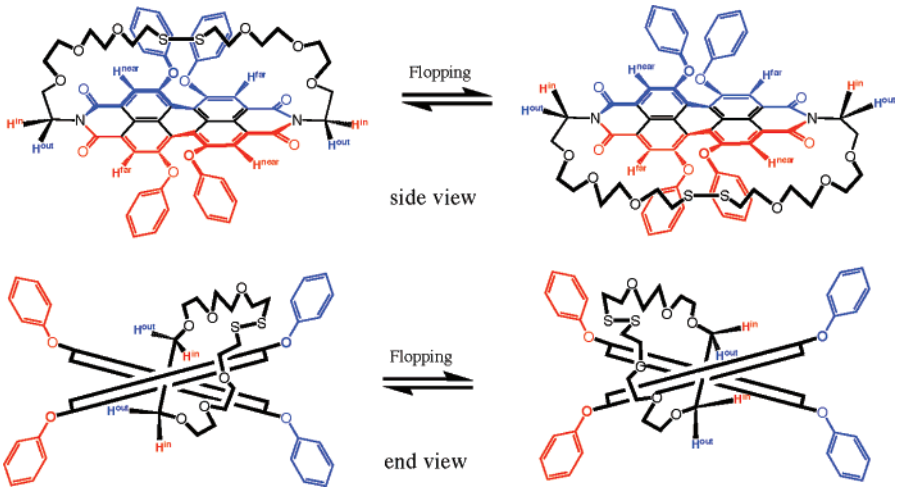

[a] The twisted perylene core is simplified into a dihedral angle for clarity in the end-view presentation.

an 8-line one. Once this basic spectral analysis is sorted out, the effect of chemical exchange on this system can easily be simulated. At the highest temperature, the two j protons become equivalent, so the spectrum becomes a simple triplet, due to the two equal couplings to the i protons. The equality of the i−j couplings indicates that there must be motion, so that the dihedral angles (and hence the couplings) between the i and j protons are averaged in some way.

The above analyses reveal the bridgehead region of the handle; the $CH_2^c-CH_2^d$ unit is more rigid than the middle region near the S−S bond or the $CH_2^g-CH_2^h$ or $CH_2^i-CH_2^j$ units. In other words, the chain is still moving even though the twisting of the perylene core is frozen below $T < -5$ °C. The motions can be generally classified into two types: spinning around C−C or C−O bonds; or, the whole chain flopping back and forth (Scheme 4 and Figure 6). Rotations around C−C and C−O bonds would lead to sharp triplet patterns for the ethylene units, and this is contrary to the experimental data. Thus, the experimental data rule out rapid and free rotation of the ethylene units. A corollary of this conclusion leads to the flopping motion of the handle using the $N-CH^c_2$ bond as an axis, which is also aligned along the long axis of the perylene core. The bulky phenoxy groups stop the handle in each case as shown in Figure 6, consistent with the fact that the handle is attempting to do a "jump-rope" but available energy at RT (or $T \leq$ RT) is insufficient to drive motion to the opposite face of the perylene group. At temperatures above −15 °C, this flopping process is rapid, and protons j and g and to some extend protons f are sharp because they remain as magnetically equivalent CH_2 sets through averaging the H^a_{near} and H^a_{far} environments. Below −15 °C, the flopping motion is frozen, and j protons become magnetically inequivalent, and all the carbon atoms on the handle become prochiral. In this situation, each proton becomes magnetically inequivalent in its own way as exemplified by the bridgehead protons (c) and bridge center protons (j).

A final striking feature is that, within each ethylene unit $CH_2^e-CH_2^f$, $CH_2^g-CH_2^h$, or $CH_2^i-CH_2^j$, we observed one set of sharp triplet magnetic resonance (or proximately triplet) feature, namely, CH_2^f, CH_2^g, and CH_2^j, and one set of broad magnetic resonance peaks, CH_2^e, CH_2^h, and CH_2^i. While putting these sharp and broad peaks into the chemical structure of the bridgelike handle, $CH_2^e-CH_2^f-O-CH_2^g-CH_2^h-O-CH_2^i-CH_2^j$, a zigzag pattern emerged. This zigzag pattern of chemical resonance, CH_2^e(broad)$-CH_2^f$(sharp)$-O-CH_2^g$(sharp)$-CH_2^h$-(broad)$-O-CH_2^i$(broad)$-CH_2^j$(sharp), further suggests that *this* region of the TEG chain has, on average, adopted a zigzag structure while flopping back and forth. Those protons approaching the basket and experiencing the H^a_{near} and H^a_{far} environments show broader resonances and those protons away from the basket that experience less of the chiral environment are sharper. The zigzag pattern in measured spectra also supports the contention that the CH_2 units are not rapidly free rotating. The question becomes, then, what is the nature of motions that cause i and i′ protons to have identical or nearly identical

coupling constants to j protons? The answer is not entirely clear now, and it is the subject of future studies. Of further interest is understanding the gradient rigidity of the handle from the bridgehead position of the c protons to the bridge center region at the j protons.

Conclusion

We have demonstrated that molecular self-assemblies direct reaction pathways, and as a result, similar reactants with different affinity to self-organization lead to completely different reaction products. Rational design of molecular self-assemblies that favor formation of the desired self-organized nanostructures and discourage undesired nanostructures will lead down the proper reaction pathway and yield products that more closely resemble the desired self-organized structures. In this case, we obtained a unimoleuclar cyclophane because molecular self-assembly effects that direct the reaction pathway were absent. NMR studies of the dynamic exchange between the P and M enantiomers reveal an appreciable energetic barrier of 13.4 ± 0.5 kcal·mol^{-1} kcal/mol between them. This value is of importance in studies of the dynamic twisting of perylene systems that are otherwise difficult to measure without using the cyclophane structure.

Acknowledgment. The authors acknowledge the support of National Institute of General Medical Sciences (Grant GM065306) and the U.S. Department of Energy (DOE), Office of Basic Energy Sciences, Division of Materials Science, and Engineering Physics. A.D.Q.L. is a Beckman Young Investigator.

Supporting Information Available: Synthetic route to unimolecular perylene diimide cyclophane and GOESY assignments. This material is available free of charge via the Internet at http://pubs.acs.org.

References and Notes

(1) Amabilino, D. B.; Stoddart, J. F. *Chem. Rev.* **1995**, *95*, 2725−2828.

(2) (a) Gabriel, G. J.; Sorey, S.; Iverson, B. L. *J. Am. Chem. Soc.* **2005**, *127*, 2637−2640. (b) Neuteboom, E. E.; Van Hal, P. A.; Janssen, R. A. *Chem.−Eur. J.* **2004**, *10*, 3907−3918 and references therein. (c) Kieran, A. L.; Pascu, S. I.; Jarrosson, T.; Gunter, M. J.; Sanders, J. K. M. *Chem. Commun.* **2005**, 1842−1844. (d) Li, Z. T.; Stein, P. C.; Becher, J.; Jensen, D.; Mork, P. *Chem.−Eur. J.* **1996**, *2*, 624−633.

(3) (a) Stoddart, J. F.; Tseng, H.-R. *Proc. Natl. Acad. Sci. U.S.A.* **2002**, *99*, 4797−4800. (b) Raehm, L.; Kern, J.-M.; Sauvage, J.-P.; Hamann, C.; Palacin, S.; Bourgoin, J.-P. *Chem.−Eur. J.* **2002**, *8*, 2153−2162. (c) Kaiser, G.; Jarrosson, T.; Otto, S.; Ng, Y.-F.; Bond, A. D.; Sanders, J. K. M. *Angew. Chem., Int. Ed. Engl.* **2004**, *43*, 1959−1962. (d) Aricó, F.; Badjic, J. D.; Cantrill, S. J.; Flood, A. H.; Leung, K. C.-F.; Liu, Y.; Stoddart, J. F. *Top. Curr. Chem.* **2005**, 203−259. (e) Fuller, A. M. L.; Leigh, D. A.; Lusby, P. J.; Slawin, A. M. Z.; Walker, D. B. *J. Am. Chem. Soc.* **2005**, *127*, 12612−12619. (f) Leigh, D. A.; Lusby, P. J.; Slawin, A. M. Z.; Walker, D. B. *Angew. Chem., Int. Ed.* **2005**, *44*, 4557−4564.

(4) Wang, W.; Wang, L. Q.; Palmer, B. J.; Exarhos, G. J.; Li, A. D. Q. *J. Am. Chem. Soc.* **2006**, *128*, 11150−11159.

(5) Deng, N. L.; Marwaha, V. R.; Garcia, M. E.; Benesi, A.; Mallouk, T. E. *Tetrahedron Lett.* **1995**, *36*, 7599−7602.

(6) Garcia, M. E.; Gavin, J. A.; Deng, N. L.; Andrievsky, A.; Mallouk, T. E. *Tetrahedron Lett.* **1996**, *37*, 8313−8316.

(7) Nishimura, J.; Nakamura, Y.; Hayashida, Y.; Kudo, T. *Acc. Chem. Res.* **2000**, *33* (10), 679−686 and references therein.

(8) Das, B.; Abe, S. *J. Phys. Chem. B* **2006**, *110* (47), 23806−23811.

(9) Vignon, S. A.; Wong, J.; Tseng, H. R.; Stoddart, J. F. *Org. Lett.* **2004**, *6*, 1095−1098.

(10) Wurthner, F.; Osswald, P.; Schmidt, R.; Kaiser, T.; Mansikkamaki, H.; Konemann, M.; *Org. Lett.* **2006**, *8* (17), 3765−68.

(11) Jones, B. A.; Ahrens, M. J.; Yoon, M. H.; Facchetti, A.; Marks, T. J.; Wasielewski, M. R. *Angew. Chem., Int. Ed.* **2004**, *43* (46), 6363−6366.

(12) Wurthner, F.; Stepaneko, V.; Chen, Z.; Saha-Moller, C.; Kocher, N.; Stalke, D. *J. Org. Chem.* **2004**, *69*, 7933−9.

(13) Wurthner, F.; Sautter, A.; Schilling, J. *J. Org. Chem.* **2002**, *67*, 3037−44.

(14) Wurthner, F.; Osswald, P.; Schmidt, R.; Kaiser, T.; Mansikkamaki, H.; Konemann, M. *Org. Lett.* **2006**, *8* (17), 3765−68.

(15) Chen, Z. J.; Debije, M. G.; Debaerdemaker, T.; Osswald, P.; Würthner, F. *Chem. Phys. Chem.* **2004**, *5*, 137−140.

(16) Wang, W.; Wan, W.; Zhou, H.-H.; Niu, S.-Q.; Li, A. D. Q. *J. Am. Chem. Soc.* **2003**, *125*, 5248−5249.

(17) Wang, W.; Han, J.; Wang, L.; Li, L.; Shaw, W.; Li, A. *Nano Lett.* **2003**, *3*, 455−458.

(18) Wurthner, F.; Sautter, A.; Thalacker, C. *Angew. Chem., Int. Ed. Engl.* **2000**, *39*, 1243−1245.

(19) Kanomata, N.; Ochiaia, Y. *Tetrahedron Lett.* **2001**, *42*, 1045−1048.

(20) Bodwell, G. J.; Li, J.; Miller, D. O. *Tetrahedron* **1999**, *55*, 12939−12956.

(21) Gutowsky, H. S.; Holm, C. H. *J. Chem. Phys.* **1956**, *25*, 1228−1234.

(22) Jackman, L. M.; Cotton, F. A. *Dynamic Nuclear Magnetic Resonance Spectroscopy*; Academic Press: New York, 1975.

(23) Sandstrom, J. *Dynamic NMR Spectroscopy*; Academic Press: London, 1982.

(24) Binsch, G. A. *J. Am. Chem. Soc.* **1969**, *91*, 1304−1309.

(25) Bain, A. D.; Duns, G. J. *Can. J. Chem.* **1996**, *74*, 819−824.